

Comparative Study of Photodegradation and Metastability in Solution-Processed and Plasmatic Polysilylenes

F. Schauer,^{*1,2} N. Dokoupil,² P. Horváth,² I. Kuřitka,² S. Nešpůrek,^{2,3} J. Pospíšil³

¹ Centre for Polymer Materials, Faculty of Technology, T. Bata University, T.G. Masaryk Sq. 272, 762 72 Zlín, Czech Republic

² Faculty of Chemistry, University of Technology, Purkyňova 118, 612 00 Brno, Czech Republic

³ Institute of Macromolecular Chemistry, Academy of Sciences of the Czech Republic, Heyrovsky Sq. 2, 162 06 Prague, Czech Republic

Summary: This study deals with photodegradation and metastability of polysilylenes. Physical properties of chemically prepared poly[methyl(phenyl)silylene] and polysilylenes prepared in radio-frequency and microwave discharges are compared. The position and width of the photoluminescence band due to the main chain excitations for both materials preserve but its intensity strongly depends on the preparation conditions and changes considerably during the photodegradation. The difference in photodegradation rate of both materials is explained by their different susceptibility to silyl radical formation and reverse recombination due to the chain and side groups rigidity.

Keywords: metastability; photodegradation; photoluminescence; plasma; polymerization; polysilylenes

Introduction

Photodegradation and metastability is a widely studied phenomenon and hitherto unsolved problem in silicon (sp^3)-based and σ -bonded materials with the dimensionality changing from one dimensional (1D) polysilylenes^[1] to three-dimensional (3D) systems like amorphous hydrogenated silicon ($a\text{-Si:H}$)^[2], where 3D covalently bonded network with hydrogen as broken bond terminator and stress relieving agent is formed. The complexity of the photodegradability and/or metastability rests in many intermediate steps or chemical reactions, e.g. bond scission, crosslinking, oxidation, and bond breaking and their dynamics together with the hydrogen subsystem behaviour^[3]. As real systems are disordered, a decisive role play also the topological and energetical disorder parameters, leading, e.g., to the concepts of defect pool^[4]. Polysilylenes seem to be interesting materials for the production of near-UV electroluminescence devices (LEDs)^[5]. Their main advantage is good processability

and the possibility to modify their luminescence spectra by the chemical structure of side groups. However, the liability of polysilylenes to energetical radiation resulting in their photodegradation and metastability is one of the problems limiting their applications. Recently in^[6] we have demonstrated the feasibility of the UV LED production from plasma polysilanes. The purpose of the present paper is to compare the photodegradation and metastability of solid films of poly[methyl(phenyl)silylene] (PMPSi) prepared from solution and by plasma polymerization.

Experiment

The "standard" PMPSi (chemically synthesized) was prepared as described earlier^[7]. Films were prepared from toluene solution by spin-coating on quartz (absorption) or on Si wafer (luminescence, IR absorption). For the preparation of "plasma" PMPSi, we used radio-frequency (RF) and microwave (MW) plasma techniques. Both techniques are different in many aspects^[8], namely: (1) the excitation of the monomer and presence of the energy-carrier feed gas, (2) the electron temperature and plasma density, and (3) the ion bombardment. The CVD RF plasma reactor was a 13.56 MHz radiofrequency capacitively coupled discharge unit with maximum power 1.5 W cm^{-2} . For the film deposition, we used a mixture of hydrogen (0-60 Pa) and monomer (5-30 Pa). The substrate temperature was 80°C . In microwave plasma the feed gas (helium and/or hydrogen) was ionised and excited by microwave power in an excitation discharge chamber with the frequency of 2.45 GHz under the conditions of electron cyclotron resonance (ECR) and fed to the monomer. As input monomer material methyl(phenyl)silane (Fluka, MPS) was used.

For UV-VIS absorption, IR absorption and luminescence measurements, a Hitachi U300, a Nicolet 400 FTIR, and a Perkin-Elmer LS 55 fluorimeter, respectively, were used. For the degradation experiments, the 266 nm and 355 nm light of NdYAG laser (Continuum Minilite II) was used.

Optical absorption and photoluminescence (PL) emission spectra of both standard- and plasma-PMPSi films are given in Fig. 1. Optical absorption of standard-PMPSi consists of three bands with maxima at 338 nm ($\sigma\text{-}\sigma^*$ transitions), 276 nm ($\pi\text{-}\pi^*$ transitions in phenyl groups), and 195 nm (mainly $\pi\text{-}\pi^*$ transitions as follows from quantum chemical calculations). The luminescence spectrum shows the excitonic deactivation at about 355 nm. The fluorescence quantum efficiency is quite high, about 0.15. The excitonic PL (band with maximum at 325 nm) was observed for RF plasma-PMPSi samples prepared under the partial pressure of the monomer higher than $P_{\text{mono}} = 20 \text{ Pa}$; the maximum of the band was detected at

$\lambda = 310 \div 360$ nm depending on P_{mono} . Maxima of other bands was observed at about 260 and 225 nm; also a long-wavelength absorption tail, typical of disordered materials, was detected.

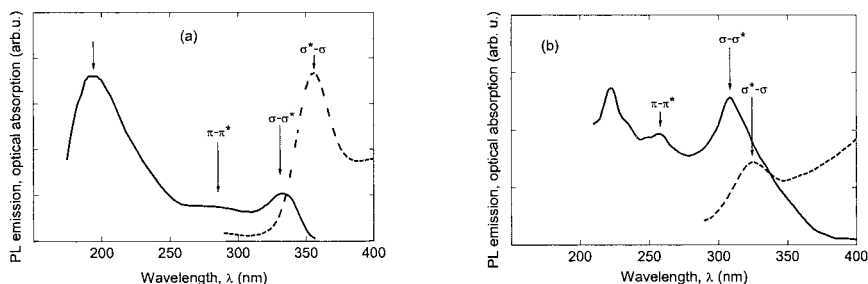


Figure 1. Absorption (full line) and emission PL ($\lambda_{\text{exc}} = 280$ nm, dotted line) spectra of (a) standard PMPSi, (b) RF plasma PMPSi ($P_{\text{mono}} = 20$ Pa, $P_{\text{H}_2} = 60$ Pa).

In Fig. 2a there are the emission spectra of standard PMPSi for different excitation wavelengths. The differences indicate that the PL spectrum consists of several components. It has been revealed that the structural defects of PMPSi, which consist not only of the branching points^[9] but also of defects produced inevitably during the polymerization and material ageing, act as radiative recombination centres for the luminescence in the visible region. In Fig. 2b this effect is depicted for the plasma PMPSi. The PL spectrum measured with $\lambda_{\text{exc}} = 280$ nm consists of both the $\sigma^*-\sigma$ exciton emission with maximum at $\lambda = 370$ nm and a broad defect luminescence centred at $\lambda \sim 480$ nm. The PL emission spectrum obtained with $\lambda_{\text{exc}} = 210$ nm differs considerably: the $\sigma^*-\sigma$ emission at $\lambda = 370$ nm is very strong and the defect luminescence is hardly observable.

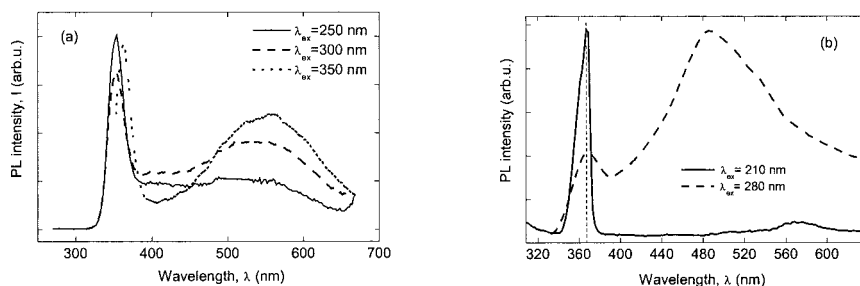


Figure 2. Emission PL spectra of (a) standard PMPSi and (b) RF plasma PMPSi; parameter is the excitation wavelength.

Degradation and stability

In Fig. 3 are compared IR spectra of standard and plasma PMPSi before and after degradation by UV radiation of 266 nm for 3600 s. There is hardly any change in bonding of phenyls in both materials after the degradation (Si-C_{ar} at 1120 and 1427 cm^{-1}), but there are changes in bonding of aliphatic carbon Si-C_{ali} (1046 and 1253 cm^{-1}). The most expressed change is the increase in absorption of the more stable $\text{Si-CH}_2\text{-Si}$ units (1039 - 1050 cm^{-1}) and subsequent formation of Si-C units near 800 cm^{-1} in both materials.

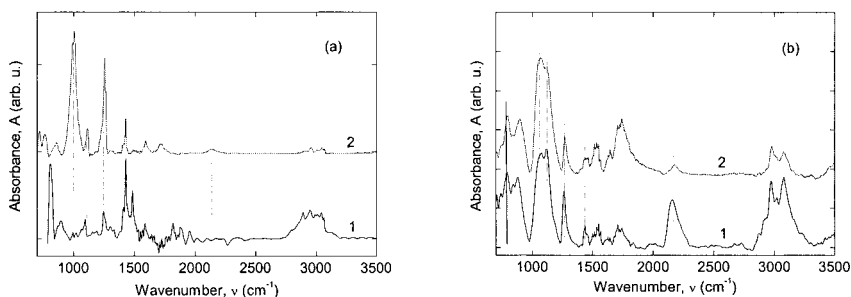


Figure 3. IR spectra of (a) standard and (b) RF plasma PMPSi before and after degradation with 266 nm light.

The scission of the Si-Si bonds of the main chain was confirmed by luminescence quenching. In Fig. 4a there is a spectral dependence of the luminescence emission of as-prepared and degraded (1 h, $\lambda_{\text{deg}} = 260$ nm) standard samples. The intensity exciton peak (A)

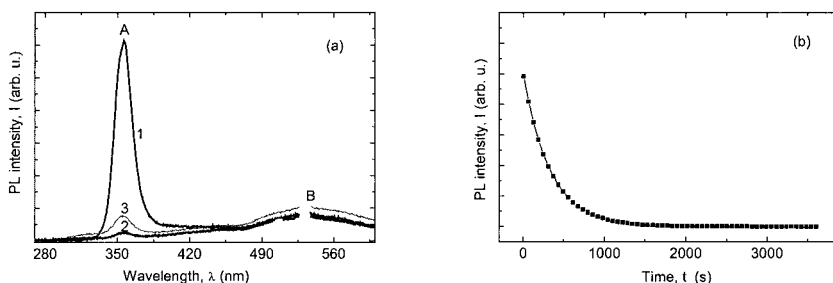


Figure 4. The quenching of the $\sigma^*\text{-}\sigma$ excitonic PL of standard PMPSi film: (a) spectral dependence, $\lambda_{\text{ex}} = 266$ nm, curve 1 – virgin sample, curve 2 – 1 h degradation with 266 nm light radiation, curve 3 – after 2 days of RT annealing; (b) time dependence of peak A.

strongly decreases with the degradation, whereas the peak of defect luminescence (B) is hardly changed. It is also remarkable that the $\sigma^*-\sigma$ peak position in luminescence (355 nm) is not changed during the degradation. In Fig. 4b is the corresponding degradation time dependence of the luminescence quenching.

We also observed remarkable changes in the dependence of the excitation spectra on degradation time ($\lambda_{\text{deg}} = 200$ nm). In Fig. 5 are excitation PL spectra detected at 360 nm for three degradation times, 0, 5 and 15 min. The most remarkable feature is a tail of the long-wavelength part of the excitation PL peak, depicting the increase of material disorder expressed by the changing slope on progressed UV irradiation. As it follows from Fig. 5b the created disorder is also wavelength-dependent. An interesting and not-explained feature of the excitation spectra is the peak near 220 nm, which decreases after UV degradation. This feature was observed also in plasma PMPSi^[10]. An additional information of this excitation anomaly comes from plasma PMPSi subjected to physical degradation by thermal treatment.

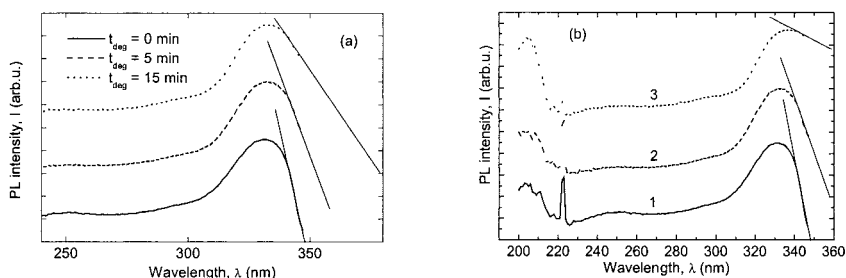


Figure 5. Excitation spectra of PL of standard-PMPSi, $\lambda_{\text{em}} = 360$ nm: (a) detail of the disorder effect, $\lambda_{\text{deg}} = 200$ nm, curve 1 – virgin sample, curve 2 – $t_{\text{deg}} = 5$ min, curve 3 – $t_{\text{deg}} = 15$ min; (b) complete excitation spectrum, curve 1 – non-degraded sample, curve 2 – $t_{\text{deg}} = 5$ min, $\lambda_{\text{deg}} = 200$ nm, curve 3 – $t_{\text{deg}} = 5$ min, $\lambda_{\text{deg}} = 325$ nm.

In effusion diagrams of plasma PMPSi, three species were observed – phenyl, CH_3 and H with corresponding temperature ranges at 400 - 500 °C, 370 - 800 °C (with maxima at 400 and 720 °C), and 500 - 800 °C, respectively. The radiative exciton photoluminescence at about 330 nm ($\lambda_{\text{exc}} = 220$ nm) strongly decreases with phenyl effusion.

Discussion

From the comparison of solution-processed and plasmatic PMPSi it may be concluded that the plasma PMPSi produced under optimised conditions is a nanostructural material with controlled 1D islands of polysilylene embedded in 3D amorphous network producing a cage effect^[6]. Its optical properties change in a broad interval, as they strongly depend on the plasma parameters. Similarity of plasma and standard PMPSi with respect to PL is well documented in Figs. 1 and 2. The PL due to σ^* - σ deexcitation preserves roughly the peak position. Similar are also absorption spectra, but the values of absorption coefficients are different, cf. $\alpha \approx 1 \times 10^4 \text{ cm}^{-1}$ vs. $1 \times 10^5 \text{ cm}^{-1}$.

Photodegradation of PMPSi films is a consequence mainly of Si–Si bond scission. From transport and charge-collection experiments follows that the photogeneration efficiency decreases with degradation^[11,12]. It is argued that the weak bond formed after irradiation and susceptible to annealing, represents the defect in conformation resulting in the recombination state and thus creating the non-radiative path for exciton trapping and deactivation. The hole transport during the photodegradation is influenced by the increase of the disorder^[13] (cf. Fig. 5.) However, the picture of the Si–Si backbone photophysics in the solid state is more complicated and it is a matter of debate. A controversy is about the absorption and scission of Si–Si bonds^[14]. There are calculations supporting various stages of deformations of Si–Si bonds. Alan et al.^[13] reported, on the basis of theoretical calculations, that the σ^* - σ transition tends to the scission of Si–Si bonds but, usually, they do not break directly because of interaction with the surrounding medium forming mainly weak Si–Si bonds^[15]. Takeda et al.^[16] found, by light-induced ESR and model calculations, two types of photocreated metastable states, one for lower photoexcitation energy (3.5 eV) due to the Si skeleton stretching and the other for higher-energy photoexcitations (4.8 eV). The weak bond concept was also used in the model of thermally activated scission with the distribution of activation energies^[17]. This model is close to the more general defect-pool model^[2] with the distributed formation energies put forward for amorphous silicon and its alloys.

Acknowledgements

This work was supported by grants from the Grant Agency of the Czech Republic (202/01/0518) and from the Ministry of Education, Youth and Sports of the Czech Republic (OC D14.30).

- [1] R.D. Miller and J. Michl, *Chem. Rev.* **1989**, 89, 1359.
- [2] R.A. Street, Hydrogenated Amorphous Silicon, Cambridge University Press, Cambridge, 1991.
- [3] N. Matsumoto, *Jpn. J. Appl. Phys.* **1998**, 37, 5425.
- [4] Z.E. Smith and S. Wagner, in *Advances in Disordered Semiconductors: Amorphous Silicon and Related Materials*, ed. H. Fritzsche, World Scientific, Singapore, N. Jersey, London, Hong Kong, 1989, pp. 409.
- [5] H. Suzuki in *Organic Electroluminescent Materials and Devices*, ed. S. Miyata and H.S. Nalwa, Gordon and Breach Publishers, 1997, p. 231.
- [6] F. Schauer, I. Kuřitka, N. Dokoupil and P. Horváth, *Physica E* 14 **2002**, 272.
- [7] F. Schauer, R. Handlir and S. Nespurek, *Adv. Mater. Opt. Electron.* **1997**, 7, 61.
- [8] N. Dokoupil, I. Kuřitka and F. Schauer, *Proc. 6th Seminary on Physics and Chemistry of Molecular Systems*, December 2000, Brno.
- [9] O. Itoh, M. Terazima, T. Azumi, N. Matsumoto, K. Takeda and M. Fujino, *Macromolecules* **1989**, 22, 10718.
- [10] P. Horváth, F. Schauer, O. Salyk, I. Kuřitka, S. Nešpůrek, J. Zemek, and V. Fidler, *J. Non-Cryst. Solids* **2000**, 266-269, 989.
- [11] R. Handlir, F. Schauer, S. Nešpůrek, I. Kuřitka, M. Weiter and P. Schauer, *J. Non-Cryst. Solids* **1998**, 227-230, 669.
- [12] O. Salyk, A. Poruba and F. Schauer, *Chem. Pap.* **1996**, 50, 177.
- [13] G. Allan, C. Delerue and M. Lannoo, *Phys. Rev. B* 48, **1993**, 7951.
- [14] H. Naito, S. Kodama, Q.Z. Kang and M. Okuda, *J. Non-Cryst. Solids* **1996**, 198-200, 653.
- [15] Y. Nakayama, T. Kurando, H. Hayashi, K. Oka and T. Dohmaru, *J. Non-Cryst. Solids* **1996**, 198-200, 657.
- [16] K. Takeda, K. Shiraishi, M. Fujiki, M. Kondo, K. Morigaki, *Phys. Rev. B* **1994**, 50, 5171.
- [17] P. Trefonas, R. West, R.D. Miller, *J. Am. Chem. Soc.* **1985**, 107, 2737.

